2003

Atomic structure, binding energy, and magnetic properties of iron atoms supported on a polyaromatic hydrocarbon

L. Senapati
Rensselaer Polytechnic Institute

S. K. Nayak
Rensselaer Polytechnic Institute

B. K. Rao
Virginia Commonwealth University

P. Jena
Virginia Commonwealth University, pjena@vcu.edu

Senapati, L., Nayak, S. K., Rao, B. K., et al. Atomic structure, binding energy, and magnetic properties of iron atoms supported on a polyaromatic hydrocarbon. The Journal of Chemical Physics 118, 8671 (2003).

Atomic structure, binding energy, and magnetic properties of iron atoms supported on a polyaromatic hydrocarbon

L. Senapati and S. K. Nayak
Department of Physics, Applied Physics, and Astronomy, Rensselaer Polytechnic Institute, Troy, New York 12180

B. K. Rao and P. Jena
Physics Department, Virginia Commonwealth University, Richmond, Virginia 23284

(Received 12 December 2002; accepted 25 February 2003)

The atomic structure, energetics, and properties of gas-phase cluster complexes containing coronene ($C_{24}H_{12}$) molecule and up to two iron atoms are studied for the first time using density functional theory and generalized gradient approximation for exchange and correlation. The geometries of the neutral and cationic iron–coronene complexes are optimized without symmetry constraint and by examining the possibility that iron atoms could occupy various sites via individual π or bridging interactions. In both neutral and cationic complexes a single Fe atom is found to preferentially occupy the on-top site above the outer ring, while two Fe atoms dimerize and reside on the top of center of the outer rings. The binding energy of neutral Fe_2–coronene defined with respect to dissociation into coronene and Fe_2 is larger than that of Fe–coronene while reverse is true for the corresponding cations. Although the ionization potentials of these complexes are not very sensitive to the number of adsorbed Fe atoms, they are significantly reduced from those of the Fe atom or the coronene molecule. The photodecomposition of cationic $(Fe_n–coronene)^+$ complexes proceeds through the ejection of either coronene$^+$ or $(Fe–coronene)^+$ cations while in the case of neutral Fe_2–coronene, the ejection of Fe_2 is energetically preferred. The coupling between the Fe atoms remains ferromagnetic although the magnetic moment/atom is reduced from the free-atom value. The results compare well with recent mass ion intensity and photofragmentation experiments. [DOI: 10.1063/1.1568077]

I. INTRODUCTION

The field of organometallic chemistry has been a topic of interest for a long time.[1] Until recently most of these studies were carried out in the solution phase. Consequently, quantitative understanding of the bonding of metal atoms to organic molecules had been difficult because of complications introduced by the solvents. These problems, however, are eliminated in gas phase studies where metal atoms produced by laser vaporization can interact only with organic molecules. Metallo-organic clusters thus formed can be mass isolated in a time of flight spectrometer and studied individually.

Considerable amount of work is available in the literature on the metal benzene (C_6H_6) complexes in the gas phase.[2] Mass ion spectroscopy and mobility experiments have suggested the existence of novel geometries with metal–benzene complexes forming either multidecker sandwich structures where metal atoms are separated by benzene molecules or ''rice ball'' structures where metal clusters are decorated with benzene molecules. Photodecomposition experiments have provided the strength of bonding in these systems while measurements of ionization potential and electron affinity illustrate their electronic structure. Comprehensive theoretical calculations are also available[3] that complement the experimental work and provide an understanding of the interaction between metal atoms and clusters with benzene molecules.

However, similar data on metal atoms adsorbed on polyaromatic hydrocarbons such as coronene ($C_{24}H_{12}$) (see Fig. 1) are rather scarce. The later group of organometallic complexes is particularly interesting since polyaromatic hydrocarbons are produced during combustion, and the interaction of these molecules with metal atoms has been suggested as a likely source of the unidentified infrared bands in the interstellar dust.[4] These molecules can also serve as a model for graphite. Thus the interaction between metal atoms and the polyaromatic hydrocarbons can shed light on the bonding of metal atoms on graphite as well as in intercalation compounds. It is only recently that monomer and dimer complexes of coronene interacting with nontransition metal ions such as Mg^+, Al^+, Si^+, In^+, Pb^+, and Bi^+, and transition metal ions (M) such as Sc^+ and Mn^+ were studied[5] in the gas phase using Fourier transform ion cyclotron resonance (FT–ICR) ion trap mass spectrometer. The bond strengths of the nontransition metal ions with coronene were found to be larger than 1.5 eV. While transition metal ions readily formed M^+ $(coronene)_2$ complexes, nontransition metal ions (Mg^+, Al^+, Si^+) did so poorly or not at all.

A detailed experimental study of the Fe–coronene complexes containing multiple Fe atoms and coronene molecules was recently carried out by Duncan and co-workers.[6] These

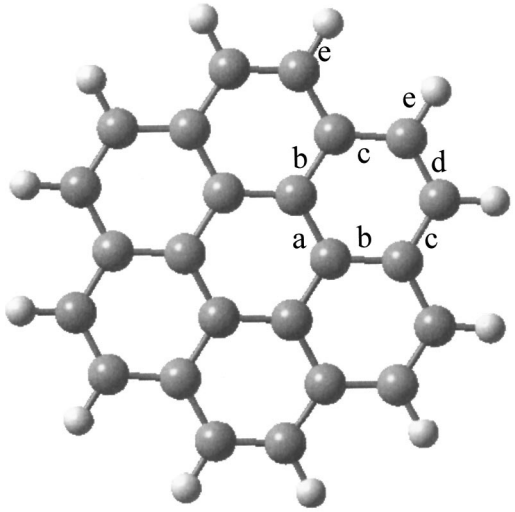

FIG. 1. Structure of coronene molecule identifying different C–C and C–H bonds. See Table I for the bond lengths.

authors measured the mass ion intensities as well as dissociation products during the photofragmentation process. Following is a summary of their findings: (1) The mass ion intensities of $(Fe_n-coronene_m)^+$ clusters continuously decrease from $(n,m)=(1,1)$ to $(n,m)=(3,1)$. No $Fe_n-coronene_m)^+$ complexes containing four or more Fe atoms were observed. (2) The mass ion intensity of $(Fe_n-coronene_m)^+$ for $(n,m)=(1,2)$ is higher than for any other complexes. This suggests that $(Fe-coronene_2)^+$ is the most stable complex and probably has a sandwich structure where the Fe atom is trapped between two coronene molecules. (3) The photodissociation of $(Fe-coronene)^+$ proceeds via its fragmentation into Fe and coronene$^+$ while $[Fe-(coronene)_2]^+$ dissociates into Fe–coronene and coronene$^+$. The former channel is consistent with the fact that the ionization potential of coronene is less than that of Fe.

Unfortunately these experiments do not provide any direct information on the structure of these complexes. For example, it is difficult to determine if the metal atoms guided by π-bonding would reside above the central or outer ring or would bind to bridge sites. It is also unclear if the structures of neutral metal–coronene complexes are the same as those of their cationic counterparts. Although it has been suggested[6] that metal atoms are dissociatively adsorbed on coronene, the evidence is not conclusive. We note that much of the structural information can only come from theoretical work. No first-principles theoretical study of the structure and properties of transition metal atoms on coronene surfaces is available to our knowledge.

In this paper we provide, what we believe to be for the first time, theoretical results on the equilibrium geometries, dissociation energies, ionization potentials, and magnetic properties of neutral and cation complexes containing iron atoms and coronene. The results are based on first-principles calculations involving density functional theory and generalized gradient approximation for exchange and correlation. In the following we give a brief description of our theoretical procedure. In Sec. III we discuss our results. A summary of our conclusions is given in Sec. IV.

II. THEORETICAL PROCEDURE

The equilibrium geometry and the total energy of coronene, Fe–coronene, and Fe_2–coronene complexes in both neutral and cationic forms are calculated using density functional theory and generalized gradient approximation for exchange and correlation. To find the ground state structure for any given complex, many starting configurations were considered. Coronene is the smallest polyaromatic hydrocarbon that resembles graphite and thus provides many sites where metal atoms can reside. To demonstrate this we refer to the structure of coronene molecule in Fig. 1. Note that a single metal atom can reside on top of the central ring, on top of any of the six outer rings, or on top of any of the four inequivalent bridge sites above a C–C bond marked by *a*, *b*, *c*, and *d* in Fig. 1. Insertion of Fe atom into the coronene plane would require major disruption of the strong C–C bond and is therefore considered unlikely. For Fe_2–coronene complexes the choices are even larger as the Fe atoms can either bind associatively (in the form of a dimer) or dissociatively (in atomic form) in addition to binding on either side of the coronene molecule. Note that for many of these structures, there is very little symmetry, so it is necessary to carry out the optimization procedure without any symmetry constraint starting from a large number of configurations.

The total energies and forces are calculated using the linear combination of atomic orbitals molecular orbital approach. We have used all electron double numerical basis (DNP[7]) for the atoms augmented by polarization functions. The DNP is comparable in quality to Gaussian 6-31G** basis set and usually yields the most reliable results. The total energies are computed using the density functional theory and generalized gradient approximation for exchange and correlation. For the latter we have used the Perdew–Wang[8] 91 form, and the computations were performed using the DMol3 code.[9] The geometries are optimized without symmetry constraint by minimizing the total energy and requiring the forces to vanish at every atom site. The threshold for these forces was set at 10^{-3} a.u./Bohr. The spin multiplicities were calculated using the aufbau principle. The calculations are repeated for neutral and cationic complexes. The vertical ionization potential is computed by calculating the energy needed to remove an electron from the neutral ground state without altering its geometry. The adiabatic ionization potential, on the other hand, represents the energy difference between the ground states of the neutral and corresponding cation.

III. RESULTS

We present our results in four steps. First, we discuss the geometry, ionization potential, and electron affinity of the coronene molecule and compare these with experiment. Similar comparisons are made for the Fe atom and the dimer. This comparison is provided to assess the accuracy of our theoretical procedure. Second, we discuss the effect of chemisorption of a single Fe atom on the electronic structure

TABLE I. Various C–C and C–H bond lengths (Å) of neutral and charged coronene molecule as well as its ionization potential and electron affinity.

Bonds	Neutral		Cation	Anion
	Theor.	Expt.		
a	1.424	1.425	1.416	1.428
b	1.426	1.433	1.428	1.436
c	1.420	1.415	1.422	1.421
d	1.376	1.346	1.382	1.382
e	1.092			
IP (eV)	7.21	7.29		
EA (eV)	0.73	0.47±0.09		

and magnetic properties of coronene followed by results of a Fe_2 supported on coronene. Finally, we analyze the effect of neglecting relaxation of coronene on the binding energies of Fe_n–coronene complexes.

A. Coronene and iron

The equilibrium structure of neutral coronene molecule as optimized in the present formulation is shown in Fig. 1. Note that there are four different kinds of C–C bonds: Bond *a* belongs to the inner ring where the first, second, and third near neighbor atoms are carbon atoms, bond *b* is the radial bond where the first two nearest neighbors are carbon atoms while the third nearest neighbor is hydrogen, bond *c* is where one of the nearest neighbor carbon atoms is bonded to hydrogen, and bond *d* is the remaining external bond where both the carbon atoms have nearest neighbor hydrogen. These bond lengths for the neutral and charged (cation or anion) coronene are listed in Table I. Note that bonds *a*, *b*, *c* have very comparable lengths namely 1.42 Å while bond *d* is significantly shorter. It is worth noting that the bond lengths of C_2 forming single, double, and triple bonds are, respectively, 1.54 Å, 1.33 Å, and 1.21 Å. Thus a bond length of 1.42 Å constitutes a bond intermediate between a single and double bond. Our results compare well with available experiment.[10]

The changes in these bond lengths as the coronene is charged by either removing or adding an electron are rather minimal. The effect of these minimal changes in both lengths on total energies can be best described by studying the vertical and adiabatic ionization potential of coronene. Note that the vertical ionization potential (VIP) measures the energy needed to remove an electron from the neutral species without changing its geometry. The adiabatic ionization potential (AIP), on the other hand, is the energy difference between the ground states of the neutral and (relaxed) cation. We see in Table II that the VIP and AIP of coronene are, respectively, 7.21 eV and 7.19 eV. Thus, the relaxation of the geometry following the electron detachment from neutral coronene only reduces the ionization potential by 0.02 eV. We will see later that similar differences exist when Fe is adsorbed. The agreement between theoretical and experimental ionization potential[11] in Table I is certainly gratifying. However, the calculated adiabatic electron affinity (i.e., the difference between the ground state energies of anion and neutral) differs from experiment[12] by about 0.2 eV. It is possible to achieve a more quantitative agreement in the electron affinity if more diffuse functions were added to the current DNP basis. However, such addition will increase computational cost considerably. Judging from the above comparison, the limit of the accuracy of our calculated energetics is about 0.2 eV.

To assess how well our results account for the properties of Fe and Fe_2, we have calculated the ionization potentials of Fe and Fe_2 as well as the binding energy and bond length of Fe_2. A considerable amount of theoretical and experimental work on Fe and Fe_2 is available[13] in the literature. Our calculated ionization potential of Fe atom of 7.64 eV agrees well with the experimental value of 7.90 eV. Similarly, our calculated binding energy and bond length of Fe_2 are 1.02 eV and 2.01 Å. Experimental values[14] of the binding energies and bond lengths of Fe_2 range between 0.61–1.28 eV and 1.73 to 2.04 Å. Thus, the agreement between theory and experiment is good, and our results on Fe–coronene complexes should have predictive capability.

B. Fe–coronene complex

In Fig. 2 we plot the geometries of the ground state and higher energy isomer of the neutral Fe–coronene complex. The geometry with the Fe atom occupying the on-top site above the outer ring [Fig. 2(a)] is the preferred structure while geometries corresponding to the on-top site above the central ring [Fig. 2(b)] is energetically higher by 0.56 eV. We attempted to optimize the structure of other possible isomers by placing the Fe atom on top of all four different bridge sites lying above bonds *a*, *b*, *c*, and *d* (see Fig. 1). None of these structures converged, and the Fe atom moved away from the bridge site towards the center of the ring site indicating that the bridge sites are unstable structures. We note that the structural change of the coronene molecule following Fe adsorption is rather minimal for all the structures studied. The ring over which Fe is adsorbed experiences its bonds stretching by only 0.02 Å. We will show later that this structural relaxation of the coronene molecule bonded to Fe

TABLE II. Total energies (a.u.) of Fe_n, coronene and Fe_n–coronene complexes corresponding to their ground state configuration. Also listed are their vertical and adiabatic ionization potentials.

Atom/cluster	Neutral	Cation	VIP (eV)	AIP (eV)
Fe	−1263.816 261	−1263.535 325	7.64	7.64
Fe_2	−2527.669 864	−2527.429 112	6.77	6.55
Coronene	−921.861 420	−921.596 922	7.21	7.19
Fe–coronene	−2185.699 060	−2185.496 559	5.69	5.51
Fe_2–coronene	−3449.570 55	−3449.366 859	5.69	5.54

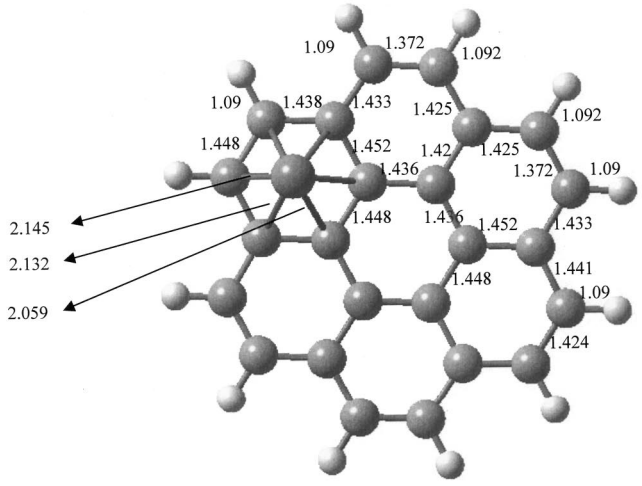

FIG. 2. (a) Ground state structure of neutral Fe–coronene complex. (b) Structure showing a higher energy isomer. The energy, ΔE is measured with respect to the ground state (a). The bond lengths (Å) following geometry optimization are listed for each case. The spin multiplicities, $M=2S+1$ are also listed.

adds very little ($\leqslant$0.1 eV) to the binding energy and can be neglected in future calculations involving multiple coronene molecules in view of the enormous savings in computer time.

Intuitively, one may not have predicted that Fe atom would prefer to reside on top of the outer ring as opposed to the central ring. To understand the origin of this preferred binding site, we plot in Fig. 3(a) the total electron charge density surface of neutral coronene corresponding to a density of 0.22 a.u. In Fig. 3(b), we plot the contour of the difference charge density surfaces corresponding to 0.005 a.u. by subtracting the superimposed atomic densities from the self-consistent total electron density. The plot, therefore, depicts the transfer of electrons from one region to another. In Fig. 3(a), we note that the electrons are confined along the bridge sites as would be characteristic of a covalently bonded system. In Fig. 3(b), the red color represents regions of deficit electrons while blue color represents regions rich with electrons. We see that the regions connecting the centers of outer rings are electron rich as is the region over the central ring. We also looked at the charge distribution from Mulliken analysis and found that the outer ring (six carbon atoms connected to outer ring have total charge of -0.18 amu) have more electrons than that of central ring (six carbon atoms connected to central ring have total charge of 0.108 amu). Since the ionization potential of Fe atom is higher than that of coronene, Fe prefers to bind to electron rich region, as it would be energetically favorable for Fe to accept rather than donate electrons. There are no direct experiments that can provide information on the equilibrium site of Fe on coronene. However, as we will show in the following, our computed energies corresponding to the ground state structures agree with experiment providing indirect evidence of the correctness of the calculated atomic structure.

The binding energy and dissociation of neutral and cationic Fe–coronene complexes into various fragments can be evaluated from the total energies corresponding to the ground state geometries listed in Table II. The dissociation energy of Fe–coronene, defined as the energy needed to dissociate the complex into Fe and coronene $[\Delta E=-E(\text{Fe–coronene})+E(\text{Fe})+E(\text{coronene})]$, is given in Table III. For the cationic complex there are two dissociation channels. Energetically preferred channel is identified to be the one for which the energy needed to dissociate is minimum. The energy barrier against dissociation can also play a role, but we have not considered this aspect in the present paper. We note that the dissociation energy of the neutral Fe–coronene corresponding to the ground state [Fig. 2(a)] is 0.58 eV. For the $(\text{Fe–coronene})^+$ cation, the complex can dissociate into one of two channels: Fe and coronene^+ or Fe^+ and coronene. To study the energetics associated with these two channels we first had to optimize the geometry of the $(\text{Fe–coronene})^+$ complex. We again examined all possible site occupancies for Fe as done in the neutral complex. The preferred site given in Fig. 4(a) is the one where Fe is bound on top of the outer ring just as in Fig. 2(a). It lies 5.51 eV higher in energy than its neutral complex. The configuration where Fe atom resides on top of the central ring of coronene [see Fig. 4(b)] is 0.71 eV higher in energy than ground state structure of the cation. Note that various C–C bonds following the attachment of Fe change very little from their values in Table I.

We note from Table III that $(\text{Fe–coronene})^+$ prefers to dissociate into Fe and coronene^+. This agrees with experiment.[6] The above channel is preferred because the ionization potential of coronene is about 0.45 eV smaller than that of Fe. It is important to note that the bond strength of $(\text{Fe–coronene})^+$ is much larger than that of the neutral since the energy needed to dissociate it is 2.27 eV while that of the neutral is only 0.58 eV. There are no experimental values of the dissociation energies of either neutral or cation Fe–coronene complex available to compare with our calculation. However, in a separate experiment Duncan and co-workers[15] have noted that photodecomposition of benzene–Fe–coronene cation yielded Fe–coronene cation. This suggests that the binding energy of Fe–coronene cation must be larger

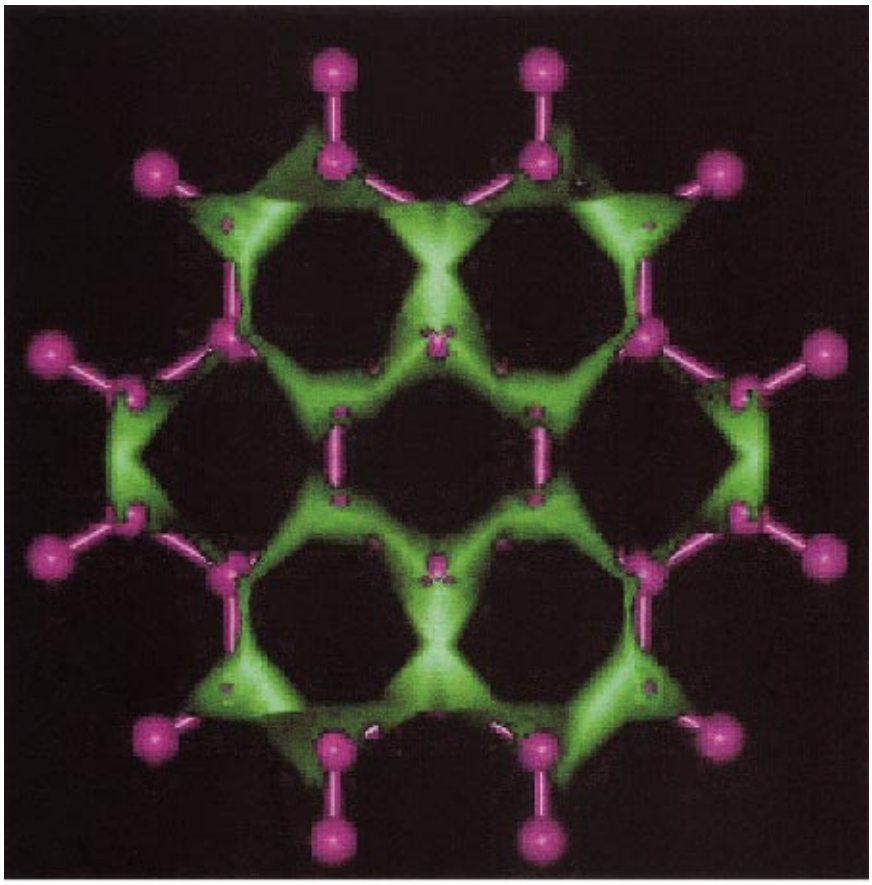

(a)

FIG. 3. (Color) (a) Constant total electron density surfaces corresponding to a density of 0.22 a.u. on the coronene plane. The green corresponds to electron-rich and red to electron deficient regions.

than that of Fe–benzene cation. Since the experimental dissociation energy of Fe–benzene cation[16] is 2.15 eV, one can only conclude that the dissociation energy of Fe–coronene cation must be larger than 2.15 eV. This is consistent with our result in Table III. Second, it was noted experimentally[6] that while Fe–coronene cation formed readily, it was difficult to synthesize the neutral form which later could have been ionized for detection in the mass spectrometer. This indicates that the binding of neutral Fe–coronene is weaker than that of its cation. This is again consistent with our result in Table III.

It is worth emphasizing that the binding energy of Fe–coronene cation is about four times larger than that of neutral Fe–coronene. Similar results have been observed in metal–benzene complexes. The dissociation energies of cationic $3d$ metal–benzene complexes are consistently larger[3,6] than their neutral counterparts for all metal atoms from Sc to Ni. In particular, the experimental dissociation energy[6] of $(\text{Fe–benzene})^+$ is 2.15 eV while that of neutral is estimated to be greater than 0.7 eV. In the case of $(\text{Co–benzene})^+$ the dissociation energy is 2.65 eV while that for the neutral is only 0.34 eV. The increased binding of the cationic complex over the neutral is due to the charge polarization caused by the positive charge and is, thus, of electrostatic origin.

C. Fe_2–coronene complex

The various optimized geometries of neutral Fe_2–coronene are shown in Fig. 5. Figure 5(a) depicts the lowest energy structure where the two Fe atoms are bound to the outer ring and reside above the center of the two outer rings. The Fe–Fe distance here is 2.45 Å which is slightly enlarged from the Fe_2 dimer bond length of 2.01 Å. Thus, one can conclude that the Fe atoms bind associatively rather than dissociatively in the neutral Fe_2–coronene complex. The energetically next higher structure is where the two Fe atoms again dimerize and bind on the outer ring over the bridge sites [Fig. 5(b)]. This lies 0.16 eV above the ground state and the Fe–Fe distance reduces to 2.22 Å. The structure in Fig. 5(c) lies about 0.59 eV above the ground state and the Fe–Fe bond length of 2.18 Å is slightly larger than that in the Fe dimer. The structures where Fe atoms are truly dissociated are exemplified by Figs. 5(d) and 5(f) which lie 0.89 eV and 0.98 eV above the ground state, respectively. The other structure where Fe atoms are bound on top of the central and outer rings [Fig. 5(e)] is nearly degenerate with Fig. 5(d), but lies 0.90 eV above the ground state. We also note from Fig. 5 that irrespective of whether Fe atoms are bound associatively or dissociatively, the stretching of the C–C

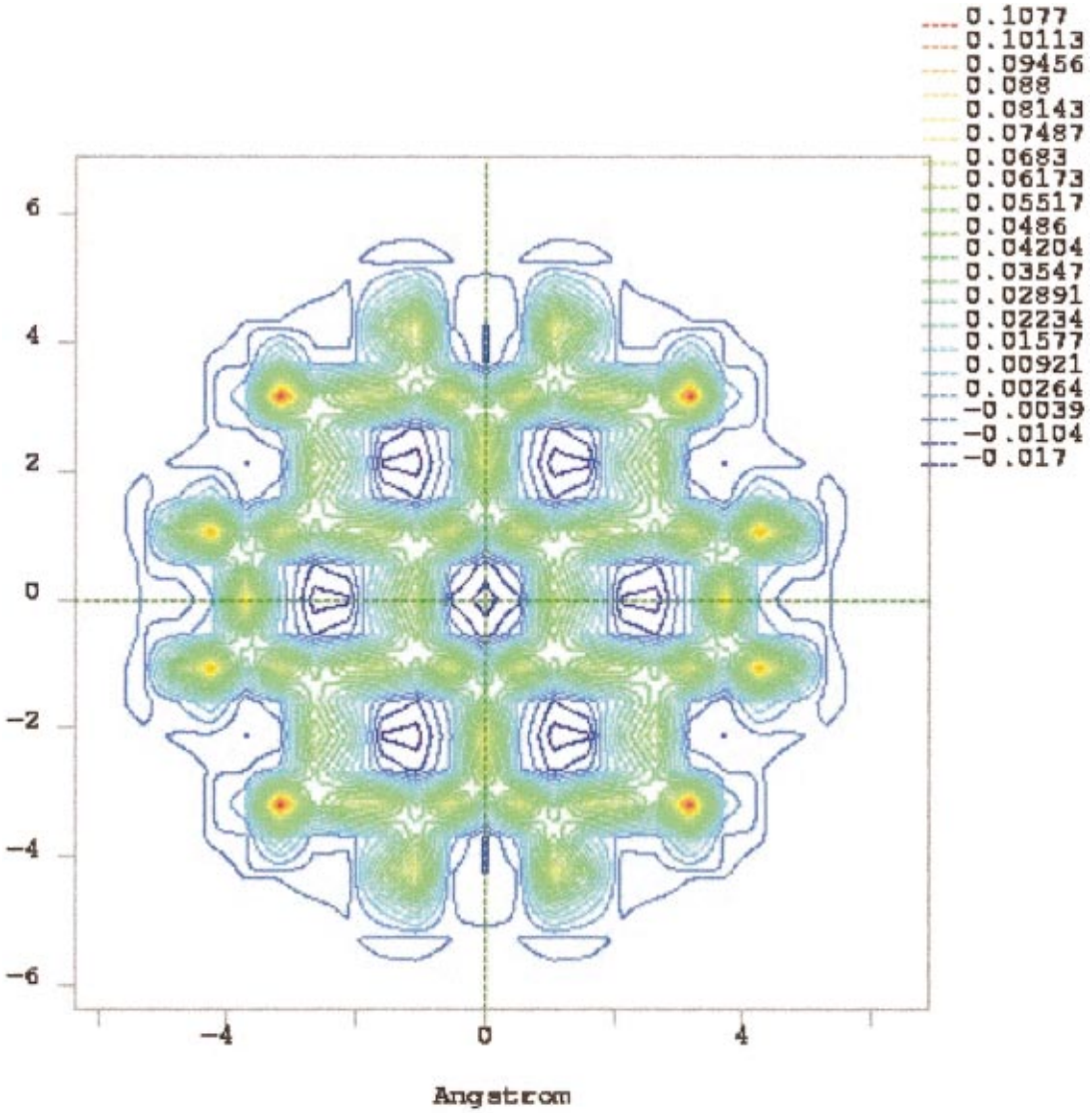

(b)

FIG. 3. (Color) (b) Difference density surfaces giving charge transfer in neutral coronene. The blue color corresponds to 0.017 a.u. electron-rich and red corresponds to 0.107 a.u. electron-rich and red corresponds to 0.107 a.u. electron deficient. The intermediate colors fall within these two values as shown in (b).

bonds lying underneath the Fe atoms is minimal. We have also considered the structure where coronene is sandwiched between two Fe atoms and the estimated energy of this structure is ~5.16 eV above the ground state structure (not bound energetically). This suggests Fe prefer to bind on the same side of the coronene.

The dissociation energies of neutral Fe_2–coronene are given in Table III. Note that there are two channels for this dissociation to occur—one in which the dissociation products are Fe_2 and coronene while in the other the dissociation products are Fe and Fe–coronene. We find that it is energetically preferable for neutral Fe_2–coronene to dissociate into a free Fe_2 dimer and a coronene. No experimental result is available to compare with this prediction. The ionization potential of Fe_2–coronene is 5.54 eV which is very close to the value in Fe–coronene. Again, there are no experimental values to compare with our theory.

In order to study the photodissociation of $(Fe_2\text{–coronene})^+$, we have optimized its geometry in a manner similar to that of its neutral complex, i.e., without any symmetry constraint. The geometries of the ground state and its higher energy isomers are given in Figs. 6(a)–6(f), re-

TABLE III. Dissociation energy of Fe_n–coronene and $(Fe_n\text{–coronene})^+$ complexes as well as ionization potentials (vertical and adiabatic). Only results associated with the ground state configurations are given.

Complex	Dissociation product	Dissociation energy (eV)
Fe–Cor	Fe+Cor	0.58
$Fe–Cor^+$	$Fe+Cor^+$	2.27
	Fe^++Cor	2.72
Fe_2–Cor	Fe_2+Cor	1.07
	Fe+FeCor	1.50
$Fe_2–Cor^+$	$Fe+Fe–Cor^+$	1.47
	Fe_2^++Cor	2.08
	Fe_2+Cor^+	2.72
	Fe^++Fe–Cor	3.60

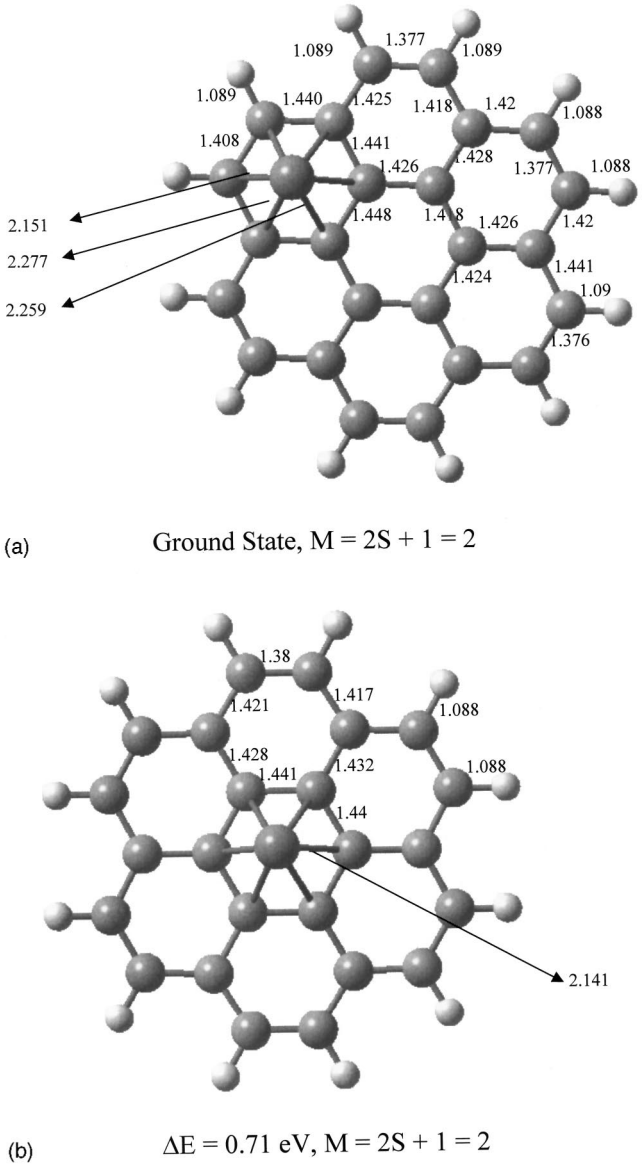

FIG. 4. Structures of Fe–coronene cation corresponding to its (a) ground state and (b) higher energy isomer. ΔE in (b) corresponds to the energy by which it lies above the ground state. The bond lengths are given in Å. The spin multiplicities, $M=2S+1$ are also listed.

spectively. The ground state geometry of the cation complex is different from its neutral with only marginal changes in the bond distances between carbon atoms and the Fe–C atoms. The ground state structure, Fig. 6(a), depicts the two Fe atoms forming a dimer and bound to the outer ring along the bridge position. The structure in Fig. 6(b) with the Fe atoms situated on top of the adjoining ring sites is only 0.01 eV above the ground state. Thus, the structures in Figs. 6(a) and 6(b) are energetically degenerate. The other isomers lie from 0.43 eV to 0.68 eV above the ground state structures in Fig. 6(a).

There are four possible channels along which $(Fe_2–coronene)^+$ can fragment. The energetics of these channels are given in Table III. The energetically most favorable path is through fragmentation into Fe and $(Fe–coronene)^+$. The energetically next favorable channel which requires 0.61 eV more energy than the above channel yields Fe_2^+ and coronene. The remaining two channels involving Fe_2 and coronene$^+$ or Fe^+ and Fe–coronene are energetically much less preferable. We note that experimentally the dissociation product is coronene$^+$ and no signal corresponding Fe_2^+ was observed. This result, at first glance, would appear to contradict our theoretical results as our calculated energy for fragmentation into Fe_2 and coronene$^+$ is 1.25 eV higher than that for fragmentation into Fe and $(Fe–coronene)^+$. As mentioned earlier, our calculations are accurate to within 0.2 to 0.3 eV. Therefore, a reason must be found to explain the above apparent discrepancy affecting photodissociation. We note that the ionization potential of coronene is about 2.8 eV higher than that of Fe–coronene. Thus, it is unlikely that the photodissociation of $(Fe_2–coronene)^+$ would yield coronene$^+$ instead of $(Fe–coronene)^+$. The likely source of this discrepancy is the possibility of multiphoton processes. It is possible that the first photon fragments $(Fe_2–coronene)^+$ to Fe and $(Fe–coronene)^+$ just as we predict, but the second photon fragments $(Fe–coronene)^+$ to Fe and coronene$^+$. And it is the latter process that is observed in the experiment.[6]

We also note that the dissociation energy of $(Fe_2–coronene)^+$ is 0.80 eV lower than that of $(Fe–coronene)^+$. This implies that the strength of binding of Fe_2 to coronene in the cationic complexes diminishes compared to that in $(Fe–coronene)^+$. It is likely that as the number of Fe_n atoms increase, their binding energy to coronene in the cationic complex will decrease until a critical limit is reached where Fe_n would prefer to remain as a free cluster. This is a likely explanation for the experimental observation that no more than three Fe atoms could be bound to coronene in the cationic configuration. Note that the neutral complexes behave differently.

D. Magnetic properties

The study of the binding of transition metal atoms to coronene brings out a feature that is not present in nontransition metal–coronene complexes. This has to do with their magnetic properties. Note that transition metal atoms, due to their localized *d* electrons, possess significant magnetic moments (i.e., unpaired spins). It is of interest to learn how the magnitude and coupling of magnetic moments of Fe atoms change as they are adsorbed on coronene. We know that in small clusters, the magnetic moment/atom of the clusters are enhanced over their bulk value,[17] although they are reduced from the free atom value of $4\mu_B$. As Fe atoms are adsorbed on metal substrates[18] or benzene,[3] their magnetic moments are reduced. While their coupling remains ferromagnetic when adsorbed on metal surfaces, they align antiferromagnetically[3] when sandwiched between benzene molecules. We have investigated this effect in Fe_n–coronene complexes by computing the spin multiplicities, $M=2S+1$ in both neutral and cationic Fe–coronene and Fe_2–coronene complexes. The spin multiplicities of Fe–coronene and Fe_2–coronene in their ground state configuration are, respectively, 3 and 7. This leads to magnetic moments of $2\mu_B$ in Fe–coronene and $6\mu_B$ in Fe_2–coronene. The results on Fe_n–coronene have both similarities as well as differences

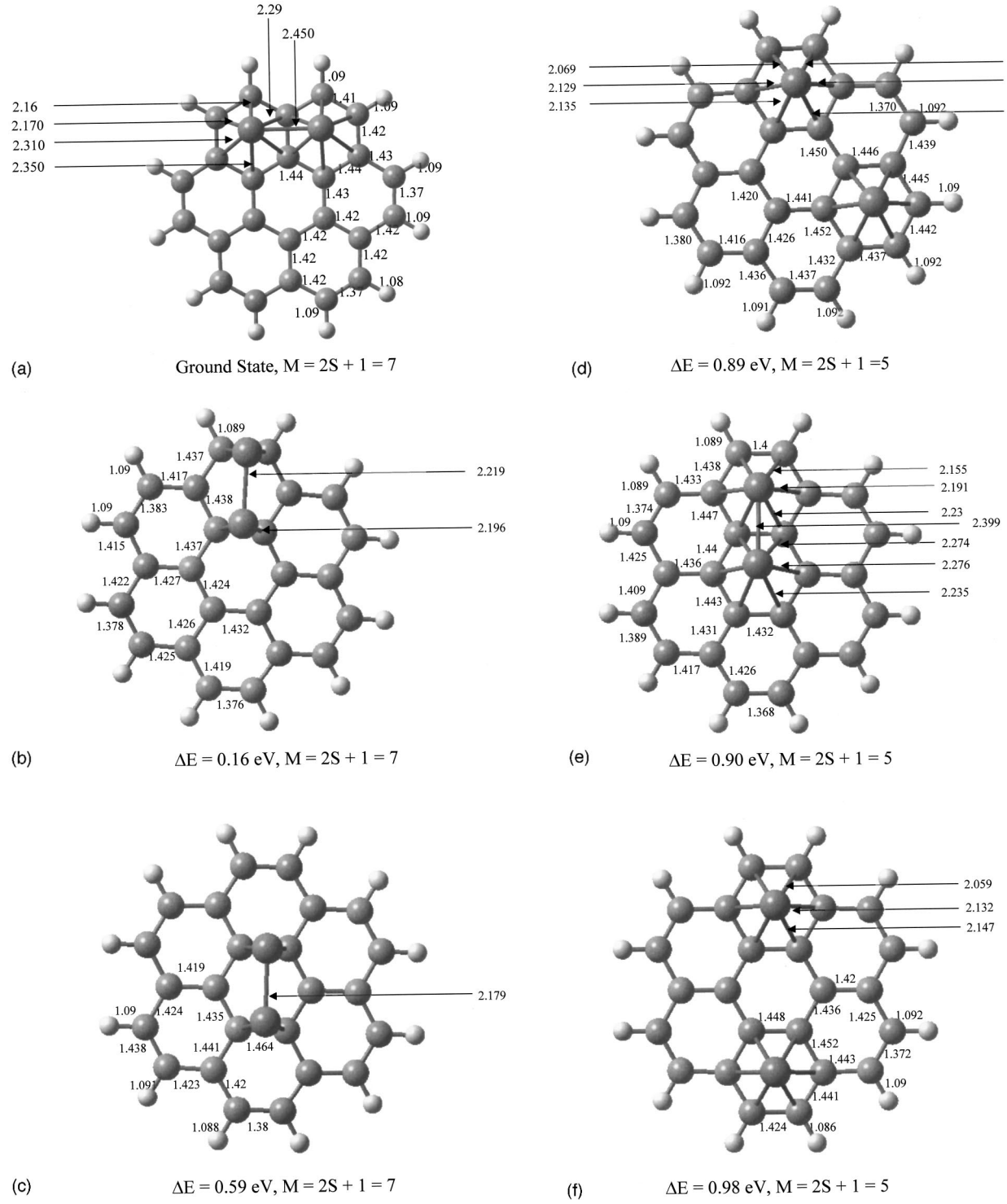

FIG. 5. Ground state and higher energy structures of neutral Fe_2 coronene complexes showing different iron bonding sites. The bond lengths (Å) following geometry optimization are listed for each case. The energies, ΔE measured with respect to the ground state (a) for higher energy isomers are given in (b)–(f). The spin multiplicities, $M=2S+1$ are also listed.

with those of Fe_n–benzene. The magnetic moment of a single Fe atom is reduced to $2\mu_B$ when adsorbed on benzene[3] just as what we have found for coronene. However, the coupling between two Fe atoms sandwiched between three benzene molecules is antiferromagnetic while it is ferromagnetic in Fe_2–coronene. It will be interesting if magnetic deflection experiments using a Stern–Gerlach field could be performed to verify our prediction.

E. Effect of relaxation of coronene on the energetics of Fe adsorption

One of the advantages of using organic molecular templates over that of metal surfaces to support atomic clusters is that metal surface atoms often relax significantly following chemisorption making theoretical studies rather difficult. Since organic molecules are characterized by covalent bond-

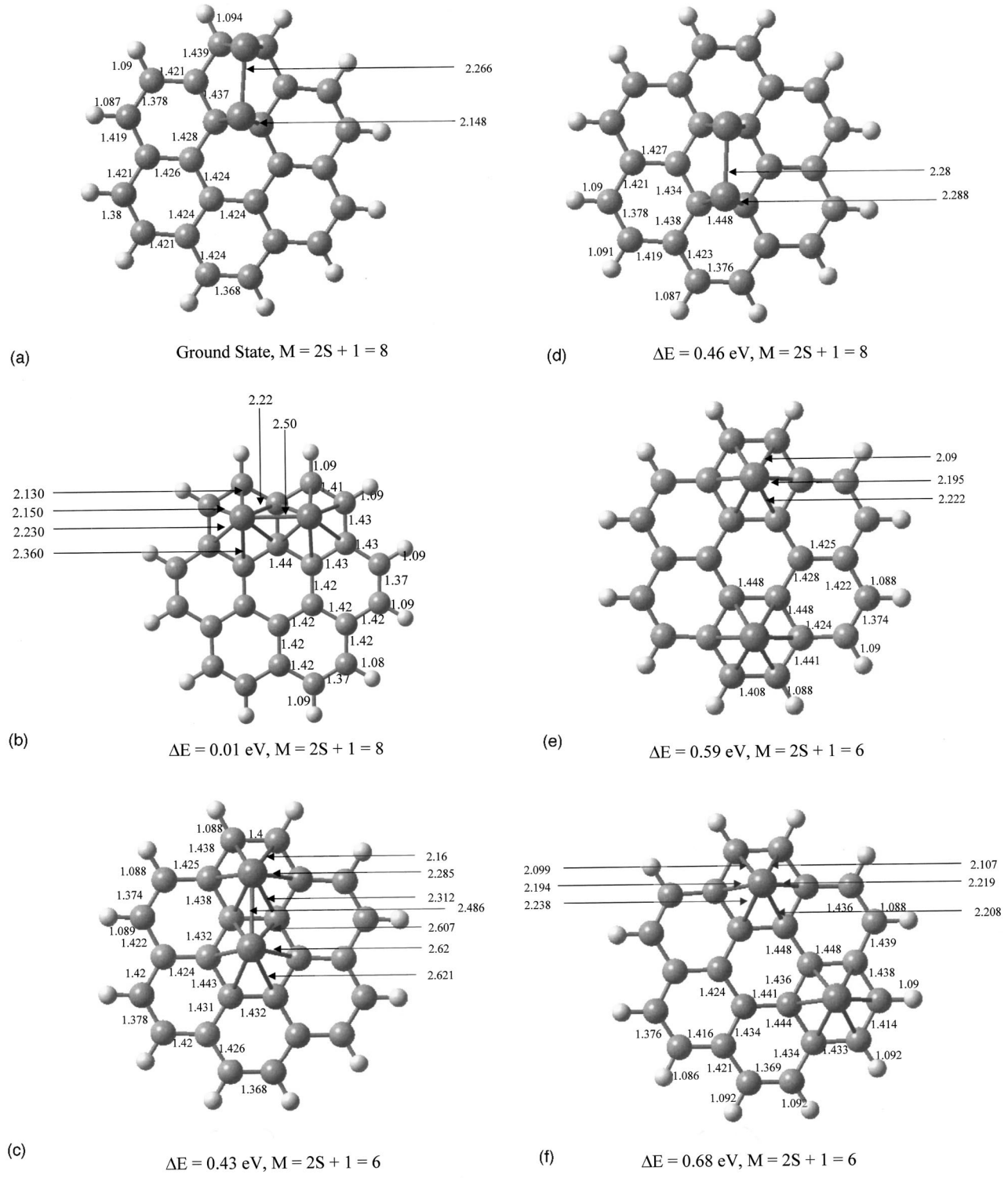

FIG. 6. Ground state and higher energy structures of Fe_2−coronene)$^+$ cation showing different iron bonding sites. The bond lengths (Å) following geometry optimization are listed for each case. The energies ΔE measured with respect to the ground state (a) for higher energy isomers are given in (b)–(f). The spin multiplicities, $M=2S+1$ are also listed.

ing that is stronger than metallic bonding, it is expected that the relaxation of the atoms in the organic molecule will be minimal. We have, indeed, seen this to be the case in Fe–coronene and Fe_2−coronene neutral and cation complexes. To examine how much energy is gained by allowing all the 36 atoms of coronene to relax as Fe clusters are deposited, we have recalculated the total energy of Fe–coronene belonging to its ground state [Fig. 2(a)] and higher energy isomer [Fig. 2(b)] by only optimizing the Fe–coronene distance while keeping all the atoms of coronene in their unperturbed configuration shown in Fig. 1. The corresponding energy differences are given in Table IV. Note that in both the ground

TABLE IV. Effect of coronene relaxation on the energetics of Fe_n adsorption. ΔE is the energy difference between fully relaxed Fe_n–coronene and the structure where coronene is not allowed to relax.

Cluster	Figure	ΔE (eV)
Fe–coronene	Fig. 2(a)	0.138
	Fig. 2(b)	0.096

state and higher energy isomer, the energy difference is only about 0.1 eV which is indeed small. This result is important as the full optimization of coronene is a very computer intensive task. Certainly optimizing the geometry of metal-clusters interacting with multiple coronene molecules at the same level done here will be prohibitive and will thus limit the size of the system one can study theoretically. The fact that the relaxation of atoms in coronene is marginal and the net resulting energy gain is minimal suggests that one can use the structure of organic molecules as it appears in its pristine configuration in obtaining geometries of larger metallocoronene complexes. This process will result in enormous savings in computer time without significantly compromising the accuracy of the predicted results.

IV. CONCLUSIONS

Using first principles total energy calculations, we show that in the neutral and cationic Fe–coronene complexes the Fe atom is π bonded to the coronene molecule lying on top of the outer ring while in the neutral and cationic Fe_2 coronene complexes, the Fe-atoms dimerize and bind preferentially to the outer ring. The binding energies of these complexes decrease with increasing Fe content in the cationic complex while the reverse is true for the neutral. The ionization potentials of these complexes are reduced substantially from individual Fe atom or coronene molecule, but remain insensitive to Fe content in Fe_n–coronene. The bond strengths of $(Fe_n\text{–coronene})^+$ are substantially larger than those in the corresponding neutral complexes and the decomposition of $(Fe_n\text{–coronene})^+$ yields either coronene$^+$ or $(Fe\text{–coronene})^+$ depending on whether $n=1$ or $n=2$. The dissociation of neutral Fe_2–coronene, however, yields different products: It fragments to Fe_2 and coronene.

The magnetic properties of Fe_n–coronene also exhibit novel behavior. The magnetic moment of Fe is quenched to $2\mu_B$ in Fe–coronene as is the case with Fe–benzene. The coupling between Fe atoms in Fe_2–coronene is ferromagnetic with a total moment of $6\mu_B$. Note that it is antiferromagnetic in multidecker Fe–benzene complexes.

It will be interesting to see how the structure and properties of the above complexes evolve as one increases the number of Fe atoms and/or coronene molecules. In particular, does the coupling between Fe atoms remain ferromagnetic? We are currently studying these systems.

ACKNOWLEDGMENTS

The authors (L.S. and S.N.) would like to thank Philip Morris, Inc. for partial support of this work while B.K.R. and P.J. acknowledge support from the Department of Energy. This work was partially supported by National Computational Science Alliance under DMR 010018N and utilized the NCSA Origin2000. We are also thankful to Professor M. Duncan for many stimulating discussions.

[1] R. S. Mulliken and W. B. Person, *Molecular Complexes* (Wiley Interscience, New York, 1969); J. C. Ma and D. A. Dougherty, Chem. Rev. **97**, 1303 (1997).
[2] T. Kurikawa, H. Takeda, M. Hirano, K. Judai, T. Arita, S. Nagano, A. Nakajima, and K. Kaya, Organometallics **18**, 1430 (1999) and references therein.
[3] C. W. Bauschlicher, H. Patridge, and S. R. Langhoff, J. Phys. Chem. **96**, 3273 (1992); R. Pandey, B. K. Rao, P. Jena, and M. A. Blanco, J. Am. Chem. Soc. **123**, 3799 (2001).
[4] L. J. Allamandola, A. G. G. M. Tielens, and J. R. Barker, Astrophys. J. Lett. **290**, L25 (1985); D. K. Bohme, Chem. Rev. **92**, 1487 (1992).
[5] B. P. Pozniak and R. C. Dunbar, J. Am. Chem. Soc. **119**, 10439 (1997).
[6] J. W. Buchanan, J. E. Reddic, G. A. Grieves, and M. A. Duncan, J. Phys. Chem. A **102**, 6390 (1998).
[7] B. Delley, J. Chem. Phys. **92**, 508 (1990).
[8] J. P. Perdew and Y. Wang, Phys. Rev. B **45**, 13244 (1992).
[9] DMol3 Code: Biosym Technologies, Inc., San Diego, CA, 1995.
[10] J. K. Fawcett and J. Trotter, Proc. R. Soc. London, Ser. A **289**, 366 (1966).
[11] See Table 1 of Ref. 6.
[12] M. A. Duncan, A. M. Knight, Y. Negeshi, S. Nagao, Y. Nakamura, A. Kato, A. Nakajima, and K. Kaya, Chem. Phys. Lett. **309**, 49 (1999).
[13] B. Nash, B. K. Rao, and P. Jena, J. Chem. Phys. **105**, 11020 (1996); M. Castro and D. R. Salahub, Phys. Rev. B **47**, 10955 (1993).
[14] D. M. Cox, D. J. Trevor, R. L. Whetten, E. A. Rohlfing, and A. Kaldor, Phys. Rev. B **32**, 7290 (1985); S. S. Lin and A. Kant, J. Phys. Chem. **73**, 2450 (1969); I. Shim and K. A. Gingerich, J. Chem. Phys. **77**, 2490 (1982); L. Lian, C. X. Su, and P. B. Armentrout, *ibid.* **97**, 4072 (1992).
[15] J. W. Buchanan, G. A. Grieves, J. E. Reddic, and M. A. Duncan, Int. J. Mass. Spectrom. **182**, 323 (1999).
[16] F. Meyer, I. A. Khan, and P. B. Armentrout, J. Am. Chem. Soc. **117**, 9740 (1995).
[17] I. M. L. Billas, A. Chatelain, and W. A. deHeer, Science **265**, 1682 (1994).
[18] K. Wildberger, V. S. Stepanyuk, P. Lang, R. Zeller, and P. H. Dederichs, Phys. Rev. Lett. **75**, 509 (1995).